NANO LETTERS

2008
Vol. 8, No. 8
2362-2368

Using Localized Surface Plasmon Resonances to Probe the Nanoscopic Origins of Adsorbate-Driven Ordering Transitions of Liquid Crystals in Contact with Chemically Functionalized Gold Nanodots

Gary M. Koenig, Jr., Brian T. Gettelfinger, Juan J. de Pablo, and Nicholas L. Abbott*

Department of Chemical and Biological Engineering, University of Wisconsin-Madison, 1415 Engineering Drive, Madison, Wisconsin 53706

Received April 25, 2008; Revised Manuscript Received June 5, 2008

ABSTRACT

We report that localized surface plasmon resonances (LSPRs) of gold nanodots immersed under liquid crystals (LCs) can be used to characterize adsorbate-induced ordering transitions of the LCs on the surfaces of the nanodots. The nanoscopic changes in ordering of the LCs, as measured by LSPR, were shown to give rise to macroscopic ordering transitions of the LCs that were observed by polarized light microscopy. The results reported herein suggest that (i) LCs may be useful for enhancing the sensitivity of LSPR-based detection of binding events and (ii) that LSPR measurements of gold nanodots provide a means to characterize the nanoscopic origins of macroscopic, adsorbate-induced LC ordering transitions.

Introduction. Surface-induced ordering of micrometer-thick films of liquid crystals (LCs) has been reported to occur on the surfaces of a wide range of organic and inorganic materials.[1–3] Although such studies reveal the ordering of the LC films to be highly sensitive to details of the structure and chemical functionality of these surfaces, the connection between the ordering of the LCs on the micrometer-scale (as probed, for example, by transmission of polarized light) and the near-surface (<20 nm) ordering of the LCs is complex and not well understood.[3–10] Nonlinear optical measurements, such as optical second harmonic generation, have yielded important insights, including observations of near-surface order above the bulk nematic-to-isotropic clearing temperatures (T_{NI}).[3,4] Such measurements, however, are complicated to perform and are not generally possible in the presence of bulk LC due to quadrupolar contributions to the second harmonic signal.[3] Molecular-level simulations have also provided important insights (e.g., that near-surface order that is less than or greater than the bulk LC can result in the same far field LC alignment),[10] but simulations are often approximate in terms of their representation of experimental systems. In this paper, we report the use of localized surface plasmon resonances (LSPRs) of gold nanodots to characterize adsorbate-induced changes in the near-surface ordering of LCs. When combined with *in situ* polarized light microscopy, we demonstrate that this simple approach permits simultaneous measurement of changes in local (nanoscopic) and far-field (bulk) ordering transitions in LCs.

LSPR-derived properties of metallic nanoparticles are known to depend on the local dielectric environment of the nanoparticles,[11–17] often giving rise to a substantial absorbance of light in the visible part of the spectrum. In the study reported in this paper, we exploit the influence of the local ordering of LCs on the dielectric environment of metallic nanoparticles to infer changes in local order via changes in the optical absorbance of the nanoparticles. By immobilizing the nanoparticles on macroscopic surfaces (referred to hereafter as nanodots), we show that it is also possible to use polarized light microscopy to simultaneously characterize changes in the far-field ordering of the LC that accompany the changes in local order of the LCs (as probed via LSPR). The ordering transitions of the LCs investigated in our study were induced by binding of dimethyl methylphosphonate

* To whom correspondence should be addressed. Tel: 608-265-5278. Fax: 608-262-5434. Email: abbott@engr.wisc.edu.

10.1021/nl801180c CCC: $40.75
Published on Web 06/26/2008

(DMMP) to the surfaces of chemically functionalized gold nanodots. The surfaces of the nanodots were functionalized (see below for details) so as to present Cu(II) ions. Past studies have demonstrated that competitive binding between the nitrile group of nematic 4-pentyl-4′cyanobiphenyl (5CB) (T_{NI} = 33.5 °C)[18] and the phosphoryl group of DMMP to Cu(II) ions supported on macroscopic gold surfaces can lead to DMMP-triggered ordering transitions in micrometer-thick films of 5CB.[19,20] In this paper, we sought to determine if we could use LSPR to detect nanoscopic changes in the ordering of the LC near the nanodot surfaces that accompany binding of DMMP. These experiments also allowed us to determine if the cooperative nature of ordering transitions in LCs can be used to enhance the LSPR response of nanodots to binding events occurring at their surfaces. In this respect, we note that DMMP is a simulant of organophosphonate nerve agents.[19] We end our introduction by commenting that there have been several past studies of LSPR phenomena in LC systems.[21–30] These past studies have not investigated adsorbate-induced ordering transitions.

Results and Discussion. The gold nanodots used in our study were prepared on the surfaces of glass substrates using methods detailed previously.[30] In brief, the methods involve physical vapor deposition of a thin film of gold onto a glass substrate, and subsequent dewetting of the film into nanodots through thermal annealing. This procedure results in arrays of nanodots with lateral dimensions of ~32 nm and heights of ~17 nm.[30] They absorb light strongly due to LSPR effects, with a peak absorbance at 551.2 ± 0.4 nm. By immersing these surface-supported nanodots into isotropic solvents that differed in refractive index from 1.33 to 1.52,[16,31,32] the refractive index sensitivities of the nanodots used in the experiments reported in this paper were determined to range from 25.7 to 28.1 nm/RIU (nanometers per refractive index unit, see Supporting Information, Figures S1, S2, and Table S1).

Our initial experiments sought to characterize the distance from the nanodot surfaces that was probed by the evanescent field of the plasmons. We used a layer-by-layer deposition method to place polyelectrolyte multilayers (PEMs) of known thicknesses over the nanodots.[33–35] The PEMs were prepared by sequential deposition of poly(allylamine) hydrochloride (PAH) and poly(acrylic acid) (PAA). We prepared PEMs on two types of samples: continuous gold films (thickness 200 nm) supported on silicon wafers and the above-described gold nanodots immobilized on glass. Self-assembled monolayers (SAMs) were formed from mercaptoundecanoic acid on both surfaces prior to deposition of the PEMs. After deposition of each PAH layer, the position of the LSPR peak was recorded on the surface presenting gold nanodots, and the ellipsometric thickness was recorded for the PEM formed on the continuous gold film (Figure 1). Inspection of the LSPR results reveals that the wavelength corresponding to the maximum absorbance of the nanodots increases with deposition of the PEM up to approximately 5 bilayers or equivalently a thickness of approximately 15 nm. Although the ellipsometric thicknesses of the PEMs were observed to increase linearly with each bilayer of polymer deposited, the

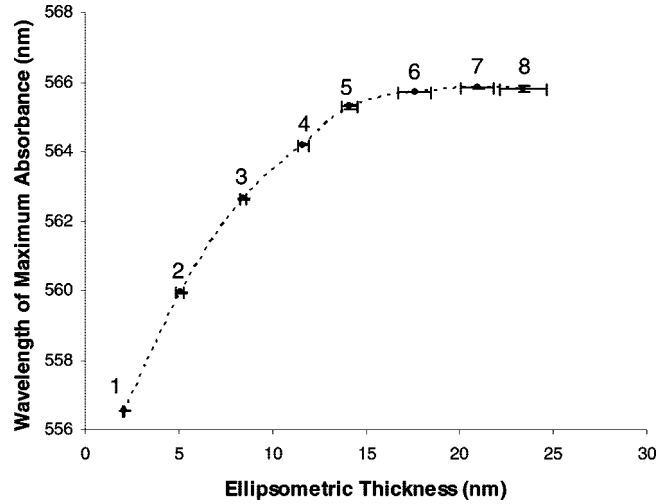

Figure 1. LSPR response of gold nanodots to deposited bilayers of PAH-PAA. The samples were measured in air and each data point corresponds to a sequentially increasing number of bilayers. Error bars represent the standard deviation of the average of five measurements.

LPSR of the nanodots was insensitive to the deposition of more than five polyelectrolyte layers. This trend is consistent with the exponentially decaying intensity of the evanescent wave with distance from the nanodot surface.[31,36] These results indicate that the nanodot-decorated surfaces used in our studies of LCs (as described below) are probing the dielectric environment created by the ordering of the LCs within approximately 15 nm of the nanodot surfaces. In contrast, surface plasmon resonance of continuous gold films is not as surface-sensitive as it is influenced by the dielectric environment within hundreds of nanometers of the gold film.[37]

Next, we prepared surface-immobilized nanodots that were functionalized sequentially with a SAM formed from mercaptoundecanoic acid and a thin layer of copper perchlorate (copper (II)/carboxylate functionalization). For the purposes of comparison, we also prepared a first reference sample that was functionalized with a SAM formed from a mixture (8:2) of decanethiol and hexadecanethiol, and a second reference sample that was functionalized with a SAM formed from hexadecanethiol. After chemical functionalization, each sample was assembled into an optical cell comprised of a 50 μm thick film of the LC 5CB that was sandwiched between the substrate supporting the functionalized gold nanodots and a piece of octyltrichlorosilane-treated glass.[30] Optical micrographs (polarized light, transmission mode using cross-polars) of the LC are shown in Supporting Information, Figure S3a−c. The optical micrographs reveal that the surfaces decorated with nanodots functionalized with either the mixed SAM formed from decanethiol and hexadecanethiol, or the Cu(II) ions, caused perpendicular (homeotropic) alignment of the bulk LC (Figure 2a). In contrast, the surfaces decorated with nanodots functionalized with SAMs formed from hexadecanethiol caused a tilted or parallel orientation of the LC,[30] consistent with alignment of bulk 5CB in the optical cell shown in Figure 2b. These orientations of the 50 μm-thick film of LC are the same as

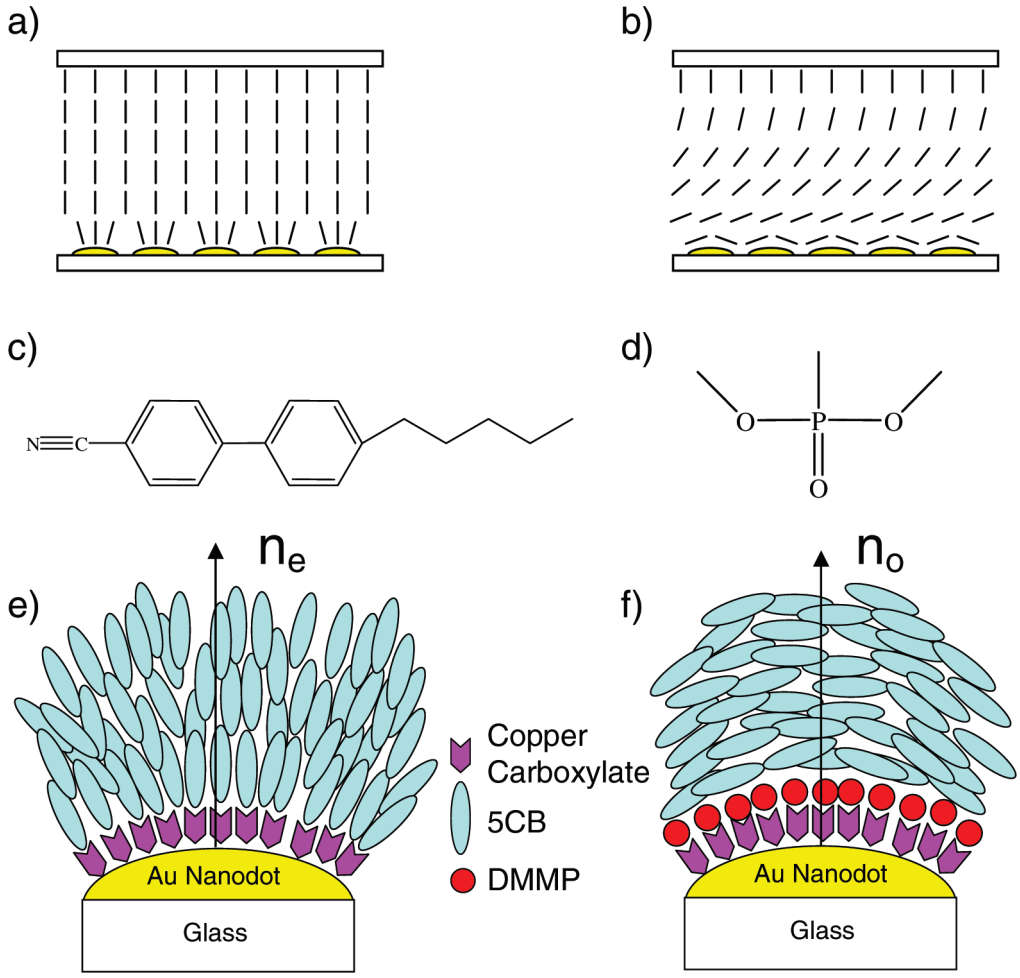

Figure 2. (a) Bulk ordering of 5CB inside an optical cell with perpendicular ordering of 5CB on both the top and bottom surfaces. (b) Bulk ordering of 5CB inside an optical cell with perpendicular ordering of 5CB at the top surface and planar ordering at the bottom surface. For panels a and b, the bottom surface presents immobilized gold nanodots and lines represent the average orientation of 5CB. Chemical structures of (c) 5CB and (d) DMMP. (e) The local ordering of 5CB near the surface of copper carboxylate functionalized gold nanoparticles, and (f) the local ordering of 5CB near the surface of copper carboxylate functionalized gold nanoparticles after exposure to DMMP. The ordering of 5CB in panel e results in the nanoparticle surface plasmon resonance being influenced by the extraordinary index of refraction (n_e) while the ordering in panel f would result in the nanoparticle being influenced by the ordinary index of refraction (n_o).

those seen when using continuous gold films with the same surface chemistry.[19,20,38–41]

In order to probe the near-surface order of the LC in contact with the above-described chemically functionalized gold nanodots (prior to exposure to DMMP), we measured the positions of the LSPR peaks of the nanodots as a function of temperature (Figure 3). If the ordering (and thus dielectric environment) of the bulk 5CB (as characterized by polarized light transmitted through the film of LC, illustrated in Figure 2a)[18] extended to the surface of the gold nanodots functionalized with Cu(II), a sharp decrease in the wavelength of the plasmon resonance at the bulk nematic-to-isotropic transition temperature of 5CB would be predicted as the local refractive index perpendicular to the nanodot surface would change from the extraordinary refractive index (1.72) to the isotropic refractive index (1.58). Inspection of Figure 3a, however, reveals that the LSPR peak position remains relatively unchanged at the bulk phase transition temperature (33.5 °C); it exhibits a slow decrease in peak wavelength with increase in temperature between 25 and 40 °C. For reference, Figure 3b shows the temperature dependence of the LSPR peak for the nanodots functionalized with the mixed SAMs, which also cause perpendicular ordering of 5CB in the bulk (optical micrographs in Supporting Information, Figure S3b and illustration of corresponding bulk alignment in Figure 2a). These measurements also reveal little change in the LSPR peak position upon heating of the bulk LC through the nematic-to-isotropic transition. In summary, these two data sets (Figures 3a,b) suggest that interactions between 5CB and the surfaces of the chemically functionalized nanodots lead to local ordering in the 5CB that does not change substantially upon melting of the bulk LC. This result is a surprising one, particularly given that the 5CB is expected to interact with these two surface chemistries through different mechanisms. Past studies have demonstrated that copper ions order 5CB at surfaces through coordination with the nitrile group of the 5CB (Figure 2c),[20] whereas the mixed SAMs formed from long and short alkanethiols likely order the 5CB through interactions between the aliphatic tails of the 5CB and the mixed SAMs.[40] In contrast to the surface chemistries that cause perpendicular ordering of bulk 5CB, the LSPR of the nanodots function-

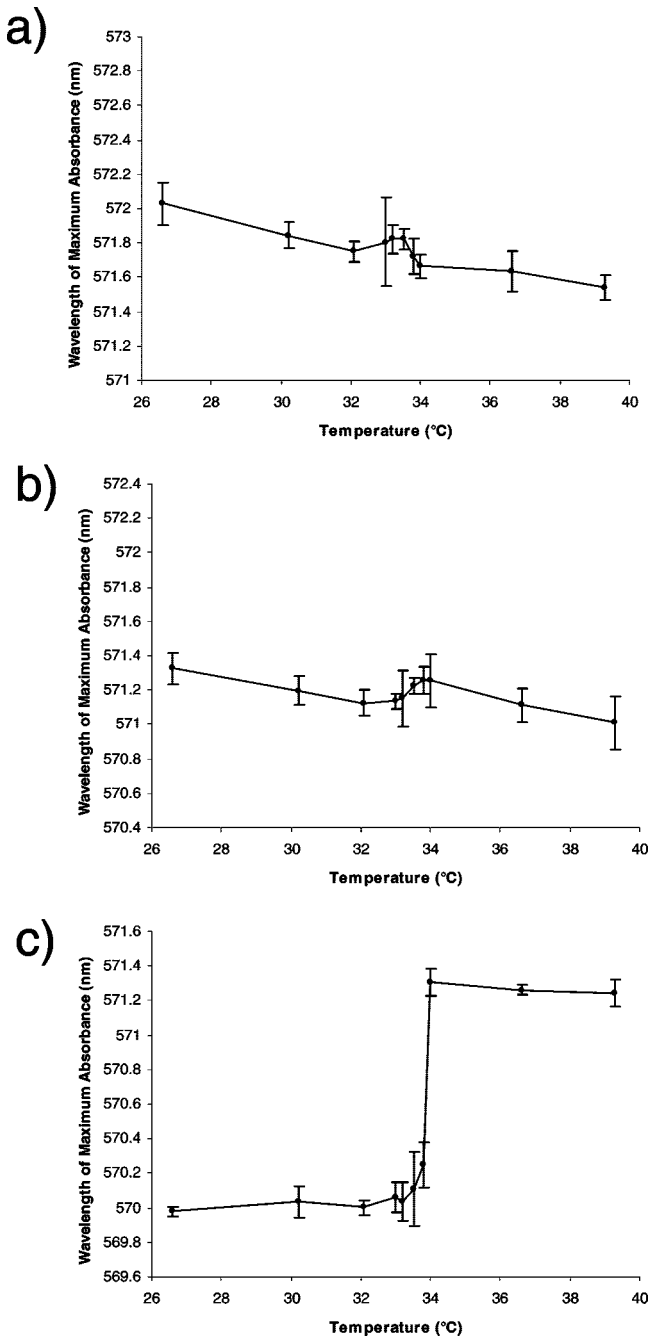

Figure 3. Characterization of temperature-dependence of the LSPR response of gold nanodots functionalized with SAMs of (a) copper carboxylate, (b) an 8:2 mixture of decanethiol:hexadecanethiol, and (c) hexadecanethiol. The measurements were performed with the nanodots immersed in 5CB. Error bars represent the standard deviation of five measurements of the same sample at the same temperature.

alized with the single component alkanethiol SAMs (which cause parallel ordering of bulk 5CB, as shown in optical micrographs in Supporting Information, Figure S3a) exhibit a substantial response at the bulk melting transition of the 5CB (Figure 3c). Inspection of Figure 3c reveals a significant increase in the LSPR peak position at the bulk nematic-to-isotropic phase transition: this red shift in the position of the LSPR peak absorbance is consistent with a change in the local refractive index near the nanodot from a value corresponding to the ordinary refractive index (1.54, as predicted for 5CB oriented parallel to the surface of nanodots) to the refractive index of isotropic 5CB (1.58). That is, for the nanodots functionalized with hexadecanethiol, the changes in the local ordering of the LC follow, at least qualitatively, changes that are also occurring in the bulk LC as a function of temperature.

In order to investigate the LSPR response caused by binding of DMMP (Figure 2d) to Cu(II) at the surfaces of the nanodots, we spread a 10 μm-thick film of 5CB over the copper carboxylate-functionalized nanodots and sandwiched the film of 5CB using a 30 μm thick membrane of poly(dimethylsiloxane) (PDMS). The PDMS film was used to form a mechanically stable film of 5CB and to allow diffusion of the DMMP from a gaseous stream to the nanodot surfaces. Figures 4a−e show polarized light photographs (crossed polars) of the copper carboxylate functionalized nanodots immersed in 5CB in the presence and absence of DMMP. Initially (Figure 4a) in air (no DMMP), the sample is dark, which is consistent with bulk perpendicular ordering of the LC with respect to the confining surfaces. After exposure to a gaseous stream of nitrogen containing 10 ppm DMMP for 40 min (Figure 4b), the entire sample is bright, which is consistent with a change in ordering of the bulk LC to so-called hybrid anchoring conditions. This anchoring refers to a situation where one surface (the PDMS) causes perpendicular ordering and the other surface (functionalized gold nanodots) promotes planar or tilted ordering of the LC (Figure 2b). Figures 4c−e demonstrate that the optical response of the LC, as measured by transmission of polarized light, is reversed upon purging the system with air free of DMMP (Figure 4c), reintroducing DMMP into the system (Figure 4d), and purging once again with air free of DMMP (Figure 4e). We note that these experiments did not attempt to maximize sensitivity or response rate to DMMP − instead, they sought to allow simultaneous measurement of the LSPR behavior of the nanodots and the ordering of the LC within the bulk of the film.

The corresponding LSPR responses of the nanodots to the presence and absence of DMMP are plotted in Figure 4f (at 24.8 °C). After exposure to 10 ppm DMMP, we measured the position of the LSPR peak to blue shift by 1.7 nm. This blue shift indicates the presence of a change in the near-surface (<15 nm) order of the LC upon exposure to DMMP. The LSPR responses of the nanodots are sensitive to the refractive index normal to the surfaces of the gold nanodots: If the local orientation of the 5CB is normal to the nanodot surface prior to exposure to DMMP (Figure 2e), then the LSPR peak will be influenced principally by the extraordinary refractive index (1.72) of the 5CB. Upon addition of DMMP, if the change in local order of the LC is similar to that described above for the bulk 5CB, the near surface orientation of the 5CB will be close to parallel to the nanodot surface (Figure 2f).[19,20] This will lead to a LSPR absorbance that will reflect the value of the ordinary refractive index of the LC. On the basis of these considerations, we calculated the maximum change in the LSPR peak position upon exposure to DMMP as the maximum change in refractive

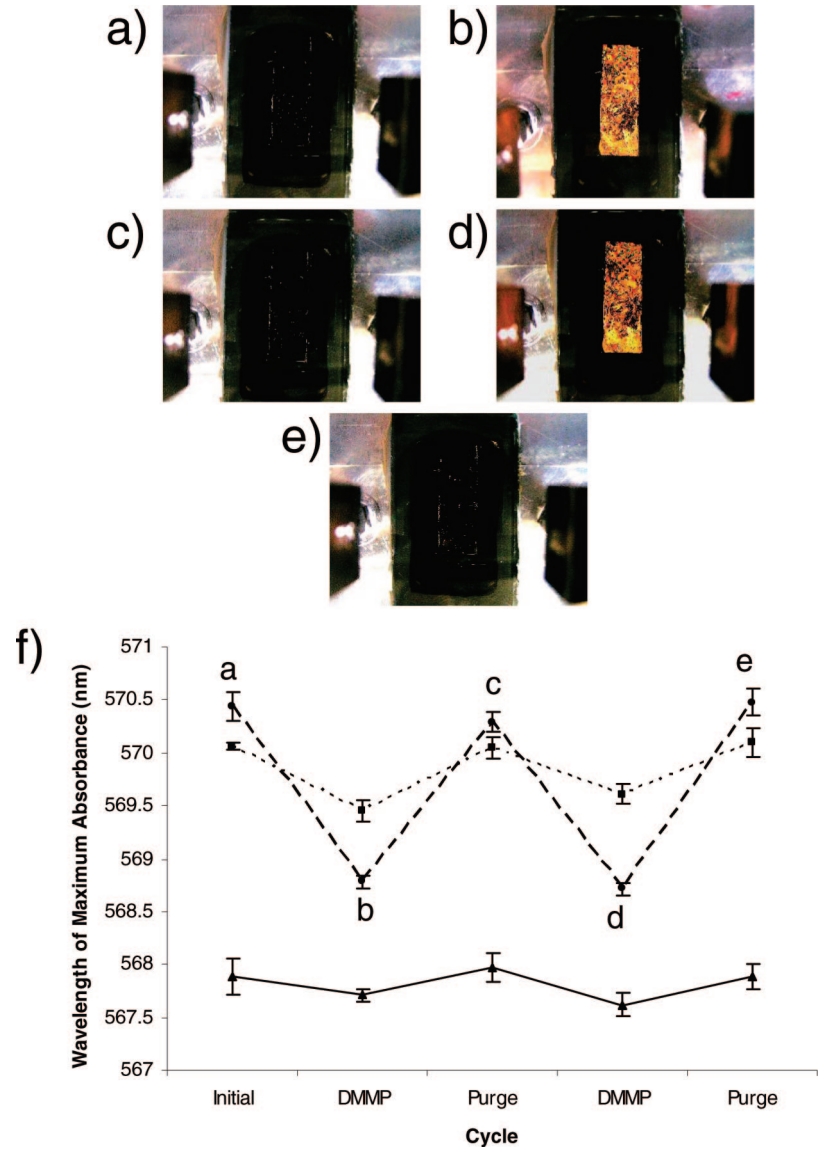

Figure 4. Optical images of nematic 5CB in contact with gold nanodots functionalized with copper carboxylate and immersed under a 10 μm film of the 5CB (a) initially in air, (b) after exposure to 10 ppm DMMP, (c) after re-exposure to air-free of DMMP, (d) after re-exposure to 10 ppm DMMP, and (e) after re-exposure to air. Polarizers were arranged orthogonally both above and below the sample and the sample was illuminated from below. The sample shown was 0.5 cm wide and 2.5 cm long. (f) (- -) LSPR responses corresponding to a−e. (▪) LSPR response to DMMP with the bulk 5CB heated into the isotropic phase. (—) LSPR response using an isotropic oil rather than 5CB.

index, −0.18, multiplied by the sensitivity of the nanodots, 28.1 nm/RIU, which corresponds to a blue shift of 5.1 nm. We note that the experimentally measured blue shift of 1.7 nm is less than the 5.1 nm calculated on the basis of the above considerations. A number of reasons likely underlie the smaller magnitude of the experimental value. The additional layer of Cu(II) perchlorate deposited onto the surface of the nanodots will make the nanodot sensitivity less than 28.1 nm/RIU. Also, the local ordering of the LC is likely not changing from being perfectly perpendicular to completely planar, which would result in an overall change in the local refractive index that is less than 0.18. Finally, the above calculation neglects the likely presence of defects within the LC near the particle surfaces.[42]

The above-described blue shift in the position of the LSPR peak absorbance upon exposure to DMMP is interesting in light of the absence of a substantial shift in the LSPR peak upon heating of the bulk 5CB through the nematic-to-isotropic phase transition (Figure 3a). As described above, we concluded that the absence of the shift in the LSPR peak upon heating was due to local ordering of the 5CB at the surface of the nanodot that persisted above the bulk phase transition. The above result obtained with DMMP supports this interpretation, as the introduction of the DMMP causes a blue shift in the LSPR response, which is consistent with a transition in the local orientation of the 5CB away from an initial state that is ordered close to the perpendicular of the nanodot surface. To provide additional insight into the nature of the change in the near-surface order upon exposure to DMMP, we heated a sample to a temperature of 41.2 °C, which is above the bulk nematic-to-isotropic transition of 5CB. Figure 4f shows the LSPR response of the sample with

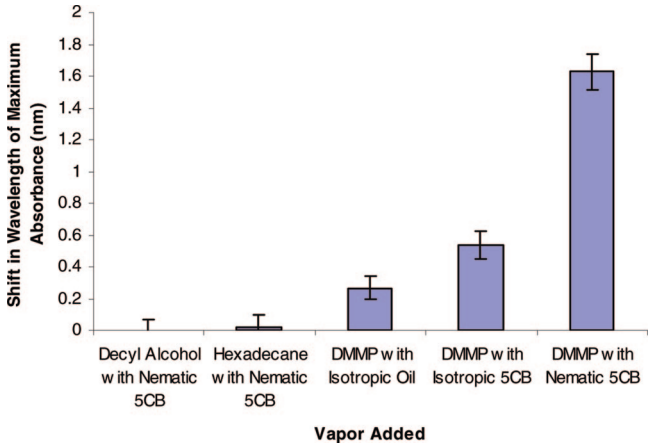

Figure 5. LSPR responses of functionalized gold nanodots to vapors of decyl alcohol, hexadecane, or DMMP. The gold nanodots were either immersed in isotropic oil, nematic 5CB, or isotropic 5CB (as indicated).

5CB in the isotropic phase, both in the absence and presence of DMMP. Upon heating to 41.2 °C and before exposure to DMMP, the LSPR peak blue-shifted by 0.4 nm (consistent with temperature effects seen in Figure 3a). After exposure to 10 ppm DMMP for 40 min, the position of the LSPR peak blue-shifted by an additional 0.6 nm (Figure 4f). The peak shifts were reversible, and the same LSPR peak positions were obtained after purging the 5CB in air for 1 h and again exposing the sample to 10 ppm DMMP. As a control, we performed an experiment where the 5CB was replaced by high refractive index (Cargille type B immersion oil with a refractive index of 1.52) isotropic oil that does not form a LC phase (Figure 4f). Inspection of Figure 4f reveals that 40 min of exposure to 10 ppm DMMP leads to a blue shift of less than 0.2 nm in the LSPR peak, which could be reversed upon purging DMMP from the system. This blue shift is consistent with binding of DMMP to the copper carboxylate surface, as DMMP has a lower refractive index (1.41) than the oil. The magnitude of the change in the position of the LSPR peak is, however, a factor of 3 less than that observed with the 5CB in the isotropic phase. These results support the conclusion that the 5CB, even when heated above the bulk 5CB phase transition temperature, is ordered at the surface of the nanodot. This ordering of the 5CB is perturbed by binding of DMMP, thus giving rise to a shift in the LSPR peak that is larger than that observed with isotropic oil.

Figure 5 shows the magnitude of the change in the LSPR peak position upon exposure to DMMP, as measured when using nematic 5CB, isotropic 5CB, and the high refractive index oil. Inspection of Figure 5 shows that the blue shift in the position of the LSPR peak induced by DMMP is 6-fold greater in 5CB as compared to the isotropic oil. As mentioned earlier, the results from Figure 1 show that the gold nanodots are sensitive to the dielectric environment within 15 nm of the particle surface. When DMMP binds to the nanodot surface in the isotropic oil, the LSPR response arises from the change in refractive index associated with a monolayer of DMMP. In contrast, when the DMMP binds to the surface of a nanodot immersed in nematic LC, reordering of the LC propagates across the entire volume probed by the evanescent waves of the nanodot. These changes in local order propagate into the bulk of the LC, as is evident in the optical textures of the LC shown in Figure 4. We conclude that LSPR provides an experimental method to characterize the nanoscopic origins of adsorbate-driven ordering transitions in LCs. We also conclude the LSPR response of nanodots to surface-binding events is substantially larger when the nanodots are immersed in LC as compared to an isotropic liquid.

Finally, we mention that we performed control experiments to confirm that the LSPR response to DMMP is surface-driven and specific to DMMP. To this end, we saturated filter paper with either liquid hexadecane or decyl alcohol and placed the impregnated filter paper into a sealed chamber with the copper carboxylate functionalized gold nanodots immersed under nematic 5CB. At 25 °C, the saturated vapor concentrations of hexadecane and decyl alcohol are ~3 and ~11 ppm, respectively. Inspection of Figure 5 reveals that the position of the LSPR peak did not change upon exposure of the LC-immersed nanodots to these organic vapors for 1 h. Additionally, the optical texture of the film of 5CB when viewed with crossed polars remained dark and did not change upon exposure to each of the organic vapors. Control experiments were also performed to confirm that the shifts in the LSPR peaks were due to DMMP binding to the Cu(II) functionalized surfaces of the nanodots as opposed to disruption of the bulk order of the LC due to dissolved DMMP (see Supporting Information, Figure S4).

Conclusions. In summary, we have reported a method to simultaneously investigate nanoscopic and bulk order of LCs during analyte-induced ordering transitions by combining the use of LSPR of gold nanodots and polarized light microscopy. Our investigation leads to two main conclusions. First, adsorbate-induced ordering transitions of LCs can be directly interrogated using LSPR, thereby providing insights into the nanoscopic changes in ordering of LCs that lead to bulk ordering transitions. Second, the cooperative nature of LC ordering transitions provides a means to amplify the LSPR responses of gold nanodots to binding events at their surfaces. The use of LSPR as a tool to probe local ordering of LCs near nanoparticles is also significant because the local order can direct the self-assembly of nanoparticles.[42,43]

Acknowledgment. The authors thank Dr. Katie Cadwell for useful discussions and suggestions and Mr. John Cannon for technical assistance. This research was partially supported by the University of Wisconsin, Nanoscale Science and Engineering Center (DMR-0425880), by DMR-0602570, and by the Army Research Office W911NF-06-1-0314.

Supporting Information Available: Sample extinction spectra for gold nanodots immersed in isotropic solvents, LSPR responses of gold nanodots with different chemical functionalizations immersed in isotropic solvents, a table summarizing the sensitivity of the gold nanodots to isotropic solvents, polarized micrographs of LCs, and DMMP control experiments. This material is available free of charge via the Internet at http://pubs.acs.org.

References

(1) Collings, P. J. *Liquid Crystals: Nature's Delicate Phase of Matter*; Princeton University Press: Princeton, NJ, 1990.
(2) Woltman, S. J.; Jay, G. D.; Crawford, G. P. *Nat. Mater.* **2007**, *6*, 929.
(3) Jerome, B. *Rep. Prog. Phys.* **1991**, *54*, 391.
(4) Chen, W.; Feller, M. B.; Shen, Y. R. *Phys. Rev. Lett.* **1989**, *63*, 2665.
(5) Ondris-Crawford, R. J.; Crawford, G. P.; Doane, J. W.; Zumer, S.; Vilfan, M.; Vilfan, I. *Phys. Rev. E* **1993**, *48*, 1998.
(6) Barberi, R.; Durand, G. *Phys. Rev. A* **1990**, *41*, 2207.
(7) Barbero, G.; Durand, G. *J. Phys. II* **1991**, *1*, 651.
(8) Papanek, J.; Martinot-Lagarde, P. *J. Phys. II* **1996**, *6*, 205.
(9) Wu, S. T.; Efron, U. *Appl. Phys. Lett.* **1986**, *48*, 624.
(10) Chiccoli, C.; Pasini, P.; Skacej, G.; Zannoni, C.; Zumer, S. *Phys. Rev. E* **2002**, *65*, 051703.
(11) Kreibig, U.; Vollmer, M. *Optical Properties of Metal Clusters*; Springer: Berlin, 1995.
(12) Link, S.; El-Sayed, M. A. *Annu. Rev. Phys. Chem.* **2003**, *54*, 331.
(13) Sun, Y.; Xia, Y. *Science* **2002**, *298*, 2176.
(14) Haes, A. J.; Haynes, C. L.; McFarland, A. D.; Schatz, G. C.; van Duyne, R. P.; Zou, S. *MRS Bull.* **2005**, *30*, 368.
(15) Kelly, K. L.; Coronado, E.; Zhao, L. L.; Schatz, G. C. *J. Phys. Chem. B* **2003**, *107*, 668.
(16) Underwood, S.; Mulvaney, P. *Langmuir* **1994**, *10*, 3427.
(17) Haes, A. J.; Van Duyne, R. P. *Exp. Rev. Mol. Diag.* **2004**, *4*, 527.
(18) Li, J.; Gauza, S.; Wu, S.-T. *J. Appl. Phys.* **2004**, *96*, 19.
(19) Shah, R. R.; Abbott, N. L. *Science* **2001**, *293*, 1296.
(20) Cadwell, K. D.; Alf, M. E.; Abbott Nicholas, L. *J. Phys. Chem. B* **2006**, *110*, 26081.
(21) Evans, P. R.; Wurtz, G. A.; Hendren, W. R.; Atkinson, R.; Dickson, W.; Zayats, A. V.; Pollard, R. J. *Appl. Phys. Lett.* **2007**, *91*, 043101.
(22) Evans, S. D.; Allinson, H.; Boden, N.; Flynn, T. M.; Henderson, J. R. *J. Phys. Chem. B* **1997**, *101*, 2143.
(23) Kieser, B.; Pauluth, D.; Gauglitz, G. *Anal. Chim. Acta* **2001**, *434*, 231.
(24) Wang, Y. *Appl. Phys. Lett.* **1995**, *67*, 2759.
(25) Wang, Y.; Russell, S. D.; Shimabukuro, R. L. *J. Appl. Phys.* **2005**, *97*, 023708.
(26) Yeatman, E. M.; Caldwell, M. E. *Appl. Phys. Lett.* **1989**, *55*, 613.
(27) Schildkraut, J. S. *Appl. Opt.* **1988**, *27*, 4587.
(28) Muller, J.; Sonnichsen, C.; von Poschinger, H.; von Plessen, G.; Klar, T. A. *Appl. Phys. Lett.* **2002**, *81*, 171.
(29) Kossyrev, P.; Yin, A.; Cloutier, S. G.; Cardimona, D. A.; Huang, D.; Alsing, P. M.; Xu, J. M. *Nano Lett.* **2005**, *5*, 1978.
(30) Koenig, G. M., Jr.; Meli, M. V.; Park, J. S.; de Pablo, J. J.; Abbott, N. L. *Chem. Mater.* **2007**, *19*, 1053.
(31) Haes, A. J.; Zou, S.; Schatz, G. C.; Van Duyne, R. P. *J. Phys. Chem. B* **2004**, *108*, 109.
(32) Larsson, E. M.; Alegret, J.; Kall, M.; Sutherland, D. S. *Nano Lett.* **2007**, *7*, 1256.
(33) Shiratori, S. S.; Rubner, M. F. *Macromolecules* **2000**, *33*, 4213.
(34) Radeva, T.; Grozeva, M. *J. Colloid Interface Sci.* **2005**, *287*, 415.
(35) Decher, G. *Science* **1997**, *277*, 1232.
(36) Doron-Mor, I.; Cohen, H.; Barkay, Z.; Shanzer, A.; Vaskevich, A.; Rubinstein, I. *Chem.—Eur. J.* **2005**, *11*, 5555.
(37) Haes, A. J.; Van Duyne, R. P. *Anal. Bioanal. Chem.* **2004**, *379*, 920.
(38) Gupta, V. K.; Abbott, N. L. *Science* **1997**, *276*, 1533.
(39) Ruths, M.; Heuberger, M.; Scheumann, V.; Hu, J.; Knoll, W. *Langmuir* **2001**, *17*, 6213.
(40) Drawhorn, R. A.; Abbott, N. L. *J. Phys. Chem.* **1995**, *99*, 16511.
(41) Miller, W. J.; Abbott, N. L. *Langmuir* **1997**, *13*, 7106.
(42) Guzman, O.; Kim, E. B.; Grollau, S.; Abbott, N. L.; de Pablo, J. J. *Phys. Rev. Lett.* **2003**, *91*, 235507.
(43) Hung, F. R.; Guzman, O.; Gettelfinger, B. T.; Abbott, N. L.; de Pablo, J. J. *Phys. Rev. E* **2006**, *74*, 011711.

NL801180C